JOURNAL OF SOLID STATE CHEMISTRY 34, 51–57 (1980)

Intergrowth in Complex Bismuth Oxides, $Bi_2CaNa_{n-2}Nb_nO_{3n+3}$ ($n = 5 \sim 8$), Revealed by 1-MV High-Resolution Electron Microscopy

SHIGEO HORIUCHI, KUNITAKA MURAMATSU, AND MASAJI SHIMAZU

National Institute for Researches in Inorganic Materials, Sakura-mura, Niihari-gun, Ibaraki, 305, Japan

Received March 1, 1979; in revised form August 9, 1979

A complex bismuth oxide crystal, prepared by heating powders with a nominal composition $Bi_2CaNb_2O_9 \cdot 4NaNbO_3$, is composed of several phases, $Bi_2CaNa_{n-2}Nb_nO_{3n+3}$, mainly with $n = 5$–8. One-megavolt high-resolution electron microscopy reveals that the structure of each phase is constructed by perovskite-like layers interleaved with Bi_2O_2 sheets. Any one of these phases grows only in limited regions, in which other phases with different values of n intergrow very finely. This causes a characteristic intensity profile on the diffraction pattern. Experimental evidence on the reaction of the crystal with water is presented.

Introduction

The crystal structure of the complex bismuth oxides, generally described as $Bi_2M_{n-1}R_nO_{3n+3}$ or $(Bi_2O_2)^{2+}(M_{n-1}R_nO_{3n+1})^{2-}$, is composed of perovskite-like layers of $M_{n-1}R_nO_{3n+1}$ and Bi_2O_2 sheets, both of which extend perpendicularly to the c axis (*1*). M represents cations like Na^+, K^+, Ca^{2+}, Sr^{2+}, Pb^{2+}, Ba^{2+}, Bi^{3+}, La^{3+}, ..., and occupies the A site in the perovskite-type structure. On the other hand, R represents the relatively smaller cations like Cr^{3+}, Fe^{3+}, Ti^{4+}, Nb^{5+}, Ta^{5+}, W^{6+}, Mo^{6+}, ..., and occupies the B site, i.e., the center of each RO_6 octahedron. As an example the structure of $Bi_2CaNb_2O_9$ ($n = 2$) is shown in Fig. 1 (*2, 3*). The symmetry is orthorhombic at room temperature. The lattice parameters a and b are almost equal to each other. The octahedra in the perovskite-like layers of $CaNb_2O_7$ are slightly tilted in rotation around the a axis (*3*). The stacking number of the octahedral sheets is identical to the value of n.

With increasing n, the perovskite-like layers become thick. It has, however, been noted that any compound of this family has $n < 5$ (*4*). It is then interesting to examine whether the compounds with $n > 5$ can really exist or not, since there are no strongly negative reasons for their formation. Ismailzade *et al.* (*5*) have prepared a series of compounds in a pseudobinary oxide system of $Bi_4Ti_3O_{12}$ and $BiFeO_3$ and reported the formation of $Bi_9Ti_3Fe_5O_{27}$ ($n = 8$). The lattice parameter in the c direction seems, however, slightly too large.

Based on a similar interest we have tried the synthesis on the system between $Bi_2CaNb_2O_9$ and $NaNbO_3$. It is our expectation that the latter component contributes to thickening of the perovskite-like layers of the former and that new phases like $Bi_2CaNa_4Nb_6O_{21}$ ($n = 6$), $Bi_2CaNa_5Nb_7O_{24}$ ($n = 7$), ..., will be formed. The latter

0022-4596/80/100051-07$02.00/0

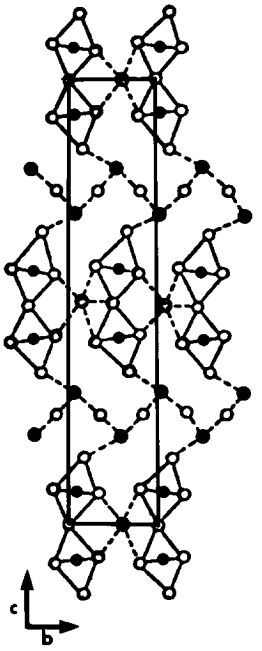

FIG. 1. Crystal structure of $Bi_2CaNb_2O_9$, viewed along the [100] direction. Large solid circles indicate Bi ions, small dark circles Nb ions, large open circles Ca ions, and small open circles O ions. The unit cell with an orthorhombic system is outlined; $a = 5.43$, $b = 5.40$, and $c = 25.15$ Å. Octahedra centered at $x = a/2$ and the corresponding Bi_2O_2 sheets are abbreviated for simplicity.

component is selected as one of the starting components because Na ions seem to best fit the *A* site on the basis of ionic size among the possible cations listed above (*4*). The specimen synthesized is composed of several phases corresponding to various values of *n* and it is difficult to definitely index the powder X-ray diffraction peaks. We therefore examined these phases by means of high-resolution electron microscopy.

The resolution limit of our 1-MV electron microscope is between 2.3 and 2.5 Å under the imaging conditions necessary for observing so-called "structure images" (*6, 7*). Accordingly the scattered waves with relatively higher diffraction angles can be used for imaging, as compared to the case of the 100-KV class electron microscope. The first merit of this is that the structure images obtained reflect the projected potential of crystal more precisely (*8*). The second merit is that it is possible to take structure images from the crystals with smaller unit cells. In some instances, this enables us to obtain structure images from more than two directions of a crystal and to determine the three-dimensional atomic array (*9*). The method has so far been successfully applied for several compounds including two kinds of complex bismuth oxide (*9, 10*).

The present study is mainly concerned with the identification of the phases and with elucidating how they are distributed in the specimen. When a 100-KV electron microscope was used in preliminary work, the specimen suffered severely from the electron irradiation even at a low magnification. At 1 MV the damage is considerably suppressed as the results below show.

Experimental Procedure

The chemical purity of both the starting powders, $Bi_2CaNb_2O_9$ and $NaNbO_3$, was 99.9%. They were mixed in a molar ratio of 1:4 and preliminarily heated at 800°C for 12 hr in air. The product was ground and the powder was molded into a disk under a pressure of 1 ton/cm^2. The disk was then heated at 1180°C for 12 hr in air. The final product was white. It was finely crushed in an agate mortar. A small fraction of the fragment powders was examined with an X-ray diffractometer. The rest was used for observation under a high-voltage electron microscope operated at 1-MV; the fragments were dispersed in a CCl_4 solution and dipped up on a holey carbon film. The adjustment and operation of the microscope were performed as reported previously (*11*). Images were taken first with a low magnification such as 30 000× together with the diffraction patterns. Some areas were photographed with a higher magnification such as 200 000×. The radius of the objective aper-

ture used corresponds to $0.60\,\text{Å}^{-1}$ in reciprocal space.

Experimental Results and Interpretation

Electron Diffraction

Crystal fragments were examined in the 1-MV electron microscope. Many diffraction patterns were taken from selected areas of about 3000 Å in diameter. It was found that several phases are formed and all of them belong to the orthorhombic system with the common lattice parameters $a = 5.51$ and $b = 5.47$ Å, the values of which are in accordance with those obtained by X-ray diffraction. The electron diffraction patterns always show streaks along the c direction. The intensity peaks in the streaks differ from one selected area to another even in a fragment of a few micrometers in size. Some examples of the patterns are represented in Fig. 2, where only the array of $00l$ reflections is shown. Figure 3 is the schematic diagram of the diffraction spots expected from the structures of $n = 5$–8. It is known from this diagram that the predominant phase corresponding to the intensity peaks in Figs. 2(a)–(d) is of $n = 5$, 6, 7, and 8, respectively. It should be noticed

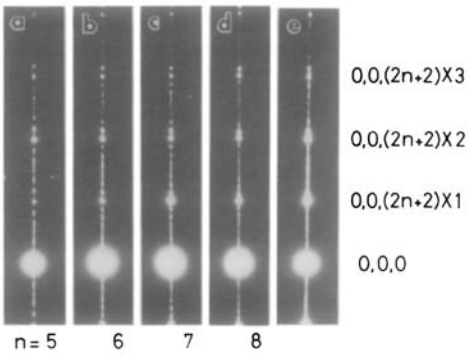

FIG. 2. Electron diffraction patterns of complex Bi oxides, $Bi_2CaNa_{n-2}Nb_nO_{3n+3}$. The predominant phase in patterns (a–d) is that of $n = 5, 6, 7$, and 8, respectively. Pattern (e) shows the close mixing of these phases. The streaks in the c direction are due to the intergrowth shown in Fig. 4.

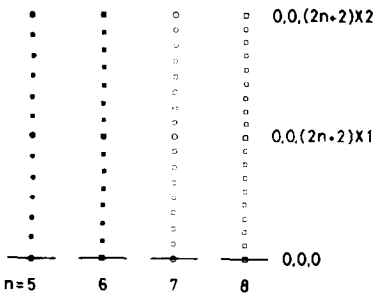

FIG. 3. Schematic array of the diffraction spots expected from the $Bi_2CaNa_{n-2}Nb_nO_{3n+3}$ phase with $n = 5$–8, respectively.

that 0, 0, $(2n+2)N$ reflections, the reciprocal lattice vectors of which are almost equal between phases, are strong in intensity, where N is an integer. The unit-cell dimension in the c direction is determined from these reflections to be 48.5 Å ($n = 5$), 56.2 Å ($n = 6$), 63.8 Å ($n = 7$), and 71.5 Å ($n = 8$). In Fig. 2(e) the intensity peaks are spaced very closely, indicating that these phases coexist in a small area with the c direction. Patterns like (a–c) and (e) are often observed with almost equal frequency, while those like (d) are observed with less frequency.

Electron Microscope Images at Low Magnification

At low magnification, only lattice fringes normal to the c axis appear. Two examples are shown. Figure 4a represents a part of the area from which the diffraction pattern in Fig. 2(c) is taken. The spacings between adjoining two fringes are mostly about 32 Å. This means formation of the phase with $n = 7$, in accordance with the indication in the diffraction pattern. The spacings are not constant in the c direction; at the parts marked the layer thickness is that of the phase $n = 6$. The diffraction streaks observed above must be due to the stacking faults as well as to the size effect relating to the intergrowth.

In most areas such a fine, syntactic intergrowth occurs very frequently. In Fig. 4b the

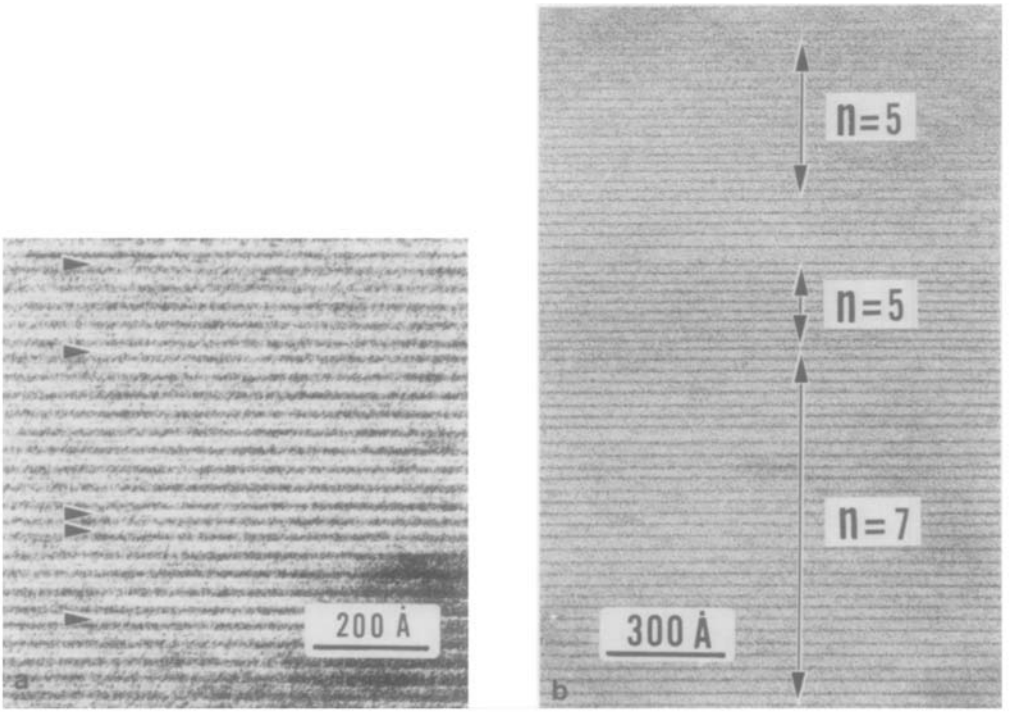

FIG. 4. Lattice fringe images taken with a 1-MV electron microscope. (a) and (b) are taken from the crystal region, giving the diffraction pattern of Figs. 2(c) and (e), respectively.

regions with a predominant phase $n = 5$ or 7 are mixed within a small scale. In each region such a syntactic intergrowth frequently occurs. In most cases the thickness of an intergrown layer differs from that of a matrix layer by about 4 Å, which corresponds to the size of perovskite subcell. The fringe spacing is occasionally very large. It is about 76 Å at most, being equal to half of the c axial dimension in the structure $n = 18$.

Structure Images

High-magnification images were then taken to examine the structure in more detail. Figure 5a is a high-resolution structure image of a thin crystal, in which the phases $n = 5$ and 6 mutually intergrow. This is taken at about 700 Å underfocus. The incident beam is normal to the common (100) plane, as is noticed from the diffraction pattern inserted. The contrast can be interpreted as follows; according to the previous observations (*9, 12*), the narrow dark bands normal to the c direction correspond to the Bi_2O_2 sheets. Bi ions are projected to form pairs and this causes the dark contrast. The layers between these are perovskite-like layers and the dark sites in them represent the Nb ions at the octahedral positions. The A sites, occupied by Ca or Na ions, are noticed as bright spots. Oxygen ions are not imaged clearly but their positions are estimated from those of the cations. This interpretation is schematically illustrated in the inset using a prototype structure model.

Figure 5b is another structure image from a different grain, in which the electron beam is incident normal to the (110) plane. The

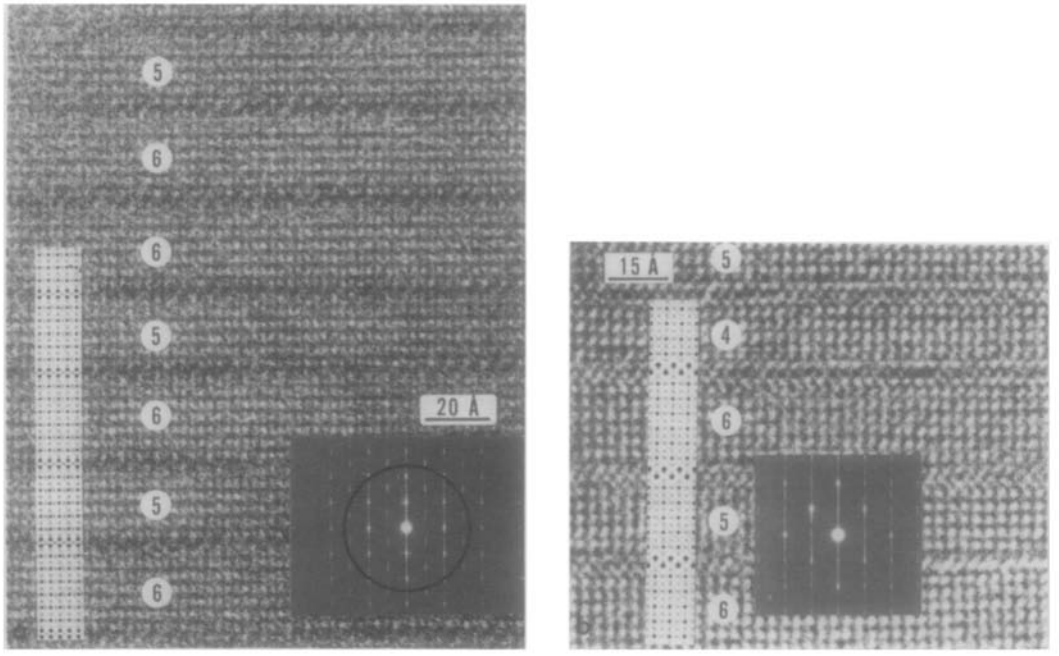

FIG. 5. One-megavolt high-resolution electron microscope images of the complex Bi oxide, $Bi_2CaNa_{n-2}Nb_nO_{3n+3}$, showing the intergrowth of the phases mainly with $n = 5$ and 6. Number indicates that of octahedra stacking along the c direction in each perovskite-like layer. The incident electron beam is normal to the (100) and (110) planes for (a) and (b), respectively. The circle on the diffraction pattern inset shows the size of the objective aperture used. The interpretation of the image contrast is illustrated by the prototype structure model. Symbols have the same meaning as those in Fig. 1 except that the large open circles indicate Na or Ca ions.

image contrast is interpretable in the same way as above. Bi ions are now imaged as dark zigzag lines running normal to the c axis. Nb ions show a dark contrast in the perovskite-like layers. The area consists of the phase $n = 4$–6. The interpretation of the image contrast is shown schematically by the prototype structure model.

In Fig. 5b the correspondence between the image contrast and the structure model is locally poor. The electron damage during observation may be partly responsible for this. Another possible reason is the chemical reaction with water occurring at the sample preparation for the electron microscopic observation, as will be explained in the next section.

Discussion

Stability of the $Bi_2CaNa_{n-2}Nb_nO_{3n+3}$ Phase

The present 1-MV high-resolution electron microscopy reveals that the complex bismuth oxide, $Bi_2CaNa_{n-2}Nb_nO_{3n+3}$, synthesized by heating the mixed powders, is mainly composed of the phases with $n = 5$–8. None of these phases grows large but they are intermixed. In each region syntactic intergrowth frequently occurs. In order to examine the stability of the state some examples were additionally prepared by the following treatments: (a) heating at 1180°C for 200 hr, (b) heating at 1260°C for 2 hr. In this case the starting powders were heated in a sealed Pt capsule to avoid the evaporation

of Bi. (c) After heating at 1180°C the product was ground. The heating and grinding process was repeated five times to achieve better homogeneity of composition. No substantial change in the structure was, however, detected in any of these samples, as compared to that mentioned in the previous sections. This presumably suggests that the minima in the free energy curves of these phases are almost equal to each other.

In order to further understand the thermodynamical relation, other compositions in the present pseudobinary oxide system must be examined. According to a preliminary experiment a similar intergrowth was observed in the specimens prepared with higher molar ratios of the same starting powders. The details will be reported elsewhere (K. Muramatsu, M. Shimazu, and S. Horiuchi, to be published).

Intensity Profile of Electron and X-Ray Diffraction

It is noted in the electron diffraction patterns (Figs. 2 and 5) that some specific reflections are strong in intensity. This is substantially due to the fact that their reciprocal lattice vectors are nearly equal to those of the perovskite subcell or the multiples.

The interference among the reflections from the matrix and the finely intergrown phases may partly contribute to intensifying the reflections; let us simplify the situation so that the matrix layers are intergrown by a different type of layer. The interference can occur when $d = \alpha/N$, where d is the lattice spacing of the matrix and α is its difference from that of the intergrown phase. For the simplest case, i.e., for the $00l$ reflections, $\alpha = 3.9$ Å and the reflections become strong when $l = (2n+2)N$.

These reflections may interfere to some extent with those of other phases, since the reciprocal lattice vectors are almost identical. This causes further intensification and especially affects the X-ray diffraction profile, in which only these strong reflections are detected clearly.

Reaction with Water

As is noted in Fig. 5b some structural changes occur when the crystal is kept in a CCl_4 solution. The figure was taken from the crystal kept in the solution for 1 day. The structural change is inappreciable in the case of the short time immersion, as Fig. 5a demonstrates. On the other hand, it becomes clearer in Fig. 6, which was taken after immersion for 20 days. The Bi_2O_2 sheets show bright contrast, indicating the destruction of the structure, while the perovskite-

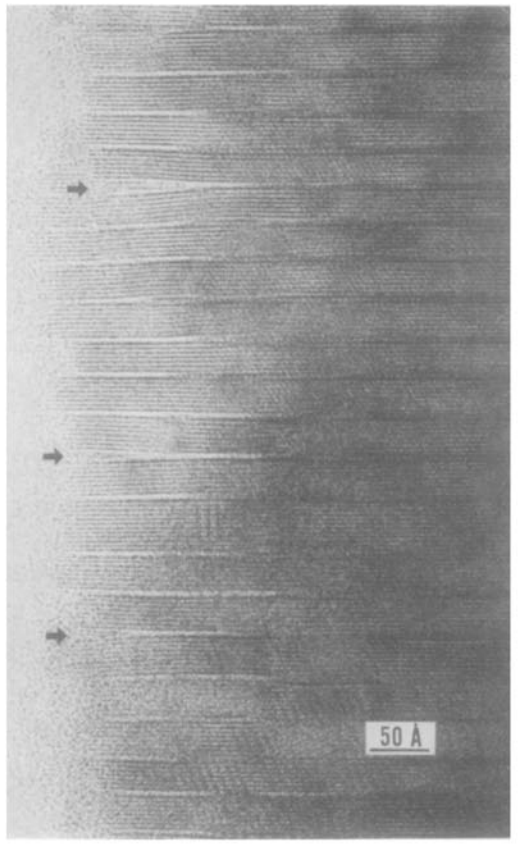

FIG. 6. A high-resolution image of a complex Bi oxide showing the structural change due to the reaction with water. The electron beam is incident normal to the (100) plane. At the parts marked cracks occur along the Bi_2O_2 sheets.

like layers remain almost unchanged. Near the edge of the fragment the layers are bent and at the parts marked cracks occur. No appreciable change is, however, detected in the diffraction pattern, probably because the structural change occurs only in the surface region of the crystal fragment.

Similar changes have not been found in other complex Bi oxides such as $Bi_7Ti_4NbO_{21}$ (*9*) or $Bi_2W_2O_9$ (*10*). A possible explanation of the present observation may be as follows; some fraction of Na or Ca ions in the crystal reacts with water which is eventually included as a trace component (0.05 wt%) in the CCl_4 solution. Because of the release of these ions from the *A* sites the perovskite-like layers slightly change in volume. This may cause the break-off of the chemical bonds between the Bi ions and their faced O ions of the perovskite-like layers, since the chemical bonding is relatively weak inherently (*3*) (as in another kind of complex Bi oxide with layer structure, $Bi_4Ti_3O_{12}$, the cleavage parallel to the (001) plane can be seen easily with the naked eye). As a result, the structure of the Bi_2O_2 sheets is no longer retained, while the structural framework of the perovskite-like layers is maintained without breakdown because of the rather strong bonding between octahedra.

In order to check the assumption some specimens kept in pure water were examined. It was found that a similar structural change occurs more rapidly.

References

1. B. AURIVILLIUS, *Ark. Kemi*, **1**, 463 (1949).
2. E. C. SUBBARAO, *J. Phys. Chem. Soc.* **23**, 665 (1962).
3. R. E. NEWNHAM, R. W. WOLFE, AND J. F. DORRIAN, *Mater. Res. Bull.* **6**, 1029 (1971).
4. M. SHIMAZU, T. KIKUCHI, AND A. WATANABE, *J. Mineral. Soc. Japan* **12**, 428 (1976).
5. I. G. ISMAILZADE, V. I. NESTERENKO, F. A. MIRISHLI, AND P. G. RUSTAMOV, *Sov. Phys. Crystallogr.* **12**, 400 (1967).
6. S. HORIUCHI, K. MURAMATSU, AND Y. MATSUI, *Acta Crystallogr. Sect. A* **34**, 939 (1978).
7. M. A. O'KEEFE, P. R. BUSECK, AND S. IIJIMA, *Nature (London)* **274**, 322 (1978).
8. S. HORIUCHI, Y. MATSUI, AND Y. BANDO, *Japan. J. Appl. Phys.* **15**, 2483 (1976).
9. S. HORIUCHI, T. KIKUCHI, AND M. GOTO, *Acta Crystallogr. Sect. A* **33**, 701 (1977).
10. Y. BANDO, A. WATANABE, Y. SEKIKAWA, M. GOTO, AND S. HORIUCHI, *Acta Crystallogr. Sect. A* **35**, 142 (1979).
11. S. HORIUCHI, Y. MATSUI, Y. BANDO, T. KATSUTA, AND I. MATSUI, *J. Electron Microsc.* **27**, 39 (1978).
12. J. L. HUTCHISON, J. S. ANDERSON, AND C. N. R. RAO, *Proc. Roy. Soc. London Ser. A* **355**, 301 (1977).